

Supporting Information for:

Surface-Amplified Ligand Disorder in CdSe Quantum Dots Determined by Electron and Coherent Vibrational Spectroscopies

Matthew T. Frederick, Jennifer L. Achtyl, Kathryn E. Knowles, Emily A. Weiss*, and Franz M. Geiger*

Department of Chemistry, Northwestern University, 2145 Sheridan Rd., Evanston, IL 60208-3113

*Corresponding authors. Email: e-weiss@northwestern.edu, geigerf@chem.northwestern.edu

Steady-State Optical Measurements. *Ground State Absorption Spectra.* We performed UV-visible absorption measurements on a Varian Cary 5000 spectrometer using 1-cm quartz cuvettes, and corrected the baselines of all spectra with neat hexanes prior to measurement.

Photoluminescence (PL) Spectra. To prepare samples for PL measurements, we diluted the QD solutions in hexanes to an optical density of <0.05 at the maximum of the first excitonic absorption of the QDs; the dilution minimized filtering effects. We collected the emission spectra on a Fluorolog-3 spectrofluorimeter (Horiba JobinYvon Spex) after exciting the samples at the peak of their second absorption maximum (see Figure S1). The emission and excitation slits passed a bandwidth of 2 nm.

Transmission Electron Microscopy (TEM). We prepared samples for TEM by applying a single drop of ~ 0.5 - μM solution of QDs in hexanes onto an ultrathin carbon TEM grid (Ted Pella, model number 814F-11019). We allowed the solvent to evaporate from the grid under ambient conditions. We observed the samples using a Jeol 2100 TEM with a 200-kV beam energy.

X-ray Photoelectron Spectroscopy (XPS). We drop-cast QDs from ~ 10 - μM hexanes solutions onto Si/SiO₂ wafers that had been cleaned with alternating rinses of acetone and ethanol, and dried in a stream of N₂. We applied eight to ten drops of solution successively to a wafer for each sample, and waited for five minutes between each drop to allow the solvent to evaporate. Prior to measurement, we stored the samples in a nitrogen atmosphere glove box to

minimize oxidation and contamination. During XPS measurements (on an Omicron ESCA Probe system), an electron flood gun at constant emission current and energy prevented the samples from charging. Scans were taken with an Al anode (1486.6 eV) driven at 225 W. We collected survey scans from binding energies of 0 - 1100 eV. For survey scans and details scans of the P(2p), Cd(3d_{3/2}) and Cd(3d_{5/2}) regions, we used a pass energy of 70 eV. Typical collection times were 10 minutes for the survey scans and 8 minutes for each of the detail scans. We averaged the detail scans over three traces of the region and analyzed four different spots on each sample. All measurements were taken at a pressure $<3 \times 10^{-9}$ mbar. The typical beam energy and emission current of the electron gun was 10 eV and 7 μ A, respectively. Binding energies (BE) were referenced to the C(1s) peak at 285.0 eV.

Figure S2 shows that the only phosphorous-containing ligands present on the QDs used for the SFG experiments are alkylphosphonates. We have found previously,¹ through ³¹P NMR experiments, that the two predominant alkylphosphonates are octylphosphonate (OPA) and *P'*-*P'*-(di-*n*-octyl) pyrophosphonate (PPA), the self-condensation product of OPA. The protonated forms of these ligands are known impurities in the reagent-grade TOPO used to synthesize the QDs.

Figures S3 and S4 show that the trend in binding energy and linewidth with radius of the QD is the same for the Cd 3d_{5/2} peak and the Cd 3d_{3/2} peak. The plot of linewidth vs. radius for the Cd 3d_{5/2} is in Figure 2 of the main text.

Age of Samples. In order to eliminate QD degradation as the cause of changes in XPS linewidth, we ran XPS experiments on two samples of QDs within 24 hours of their synthesis (the minimum time required by our cleanup procedure). The QDs with a radius of 1.9 nm (Cd/Se = 5.4:1) had an inverse Cd 3d_{5/2} linewidth of ~ 0.5 ; the QDs with a radius of 2.3 nm (Cd/Se = 2.7:1) had an inverse Cd 3d_{5/2} linewidth of ~ 0.7 . The linewidths for these samples fit on the trendline for the plot in Figure 3B, so aging the QDs in suspensions of their native ligands does not change their XPS linewidths.

Preparation of QD Films for SFG. We cleaned one-cm square, frosted glass slides by successive sonication in acetone, methanol, and distilled water for five minutes each, used a nitrogen flow to dry the slides, and placed them in an oven at 125 °C for one hour. After drying, we exposed the slides to air plasma for 1.5 min, and placed six drops of the solution of QDs in hexane (enough to cover the slides completely) on each slide and spin-coated the QD films at

2000 RPM for one minute. We deposited a second coating of QDs with the same procedure, and allowed the samples to dry in air. Figure S5 shows that residual hexanes are not responsible for the signal and that OPA is more ordered on a glass slide with no QDs present.

Determination of SFG Amplitudes. To account for the coherent nature of the experiment, the amplitudes plotted in Figure 3C were determined via spectral fitting of the relevant vibrational resonances using an Igor Pro software iterative curve fitting procedure as described previously in the literature (ref 36, 38, and 39); this procedure accounts for the proper phase relationships. Specifically, the SFG intensities occurring between 2895 cm^{-1} and 2820 cm^{-1} were fit to the sum of two interfering Lorentzians, where peak amplitude, line width, vibrational transition frequency and a constant phase were used as fitting parameters. As mentioned in reference 36 of the manuscript, the amplitudes determined with this procedure may differ from the square root of the observed SFG intensities due to the influence of the line width on the magnitude of the amplitude. Through the fitting procedure we determined that the line widths for the CH_3 and CH_2 symmetric stretching modes were similar in magnitude for large QDs (15 cm^{-1} and 15 cm^{-1} for the CH_3 and CH_2 symmetric stretching modes) but changed as the QDs became smaller to (10 cm^{-1} and 30 cm^{-1} for the CH_3 and CH_2 symmetric stretching modes). These values are comparable to the line widths and trends observed in SFG spectra, fit with similar procedures, of alkanethiols on metal nanoparticles, as discussed in reference 22 of the main text. We note that this same procedure was used to fit the SFG spectrum the OPA ligand on plain glass shown in Figure S5, which is the average of three trials to obtain the average ratio of 3.9 given in Figure 3C. A method in which raw signal intensities were used for obtaining the relevant information regarding molecular order was employed as well. In this method, the raw intensities of the CH_3 and CH_2 modes were determined by averaging the SFG intensity of five points around the central vibrational frequency, taking the square root, and then calculating the ratio of $\text{CH}_{3,\text{ss}}/\text{CH}_{2,\text{ss}}$ for each QD size, as shown in Figure S8. This analysis shows no dependence of the ratio on QD size, a result that is consistent with the fact that coherent spectra must be analyzed by phase-coupled Lorentzians as opposed to multi-peak fitting.

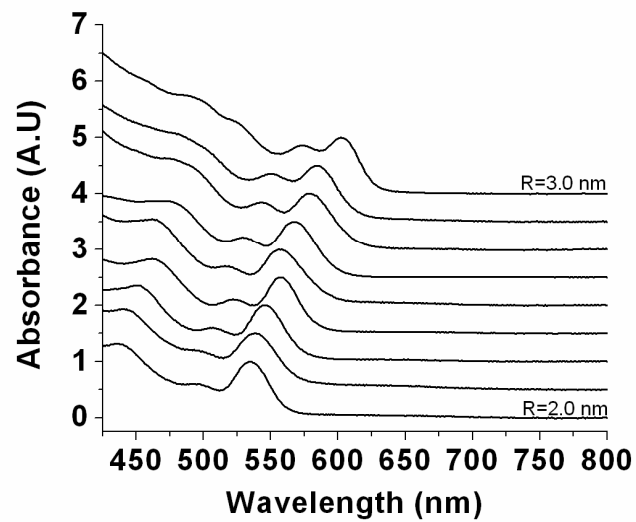


Figure S1. Ground state absorption spectra , normalized to the first absorption peak, for the QDs used in the SFG studies.

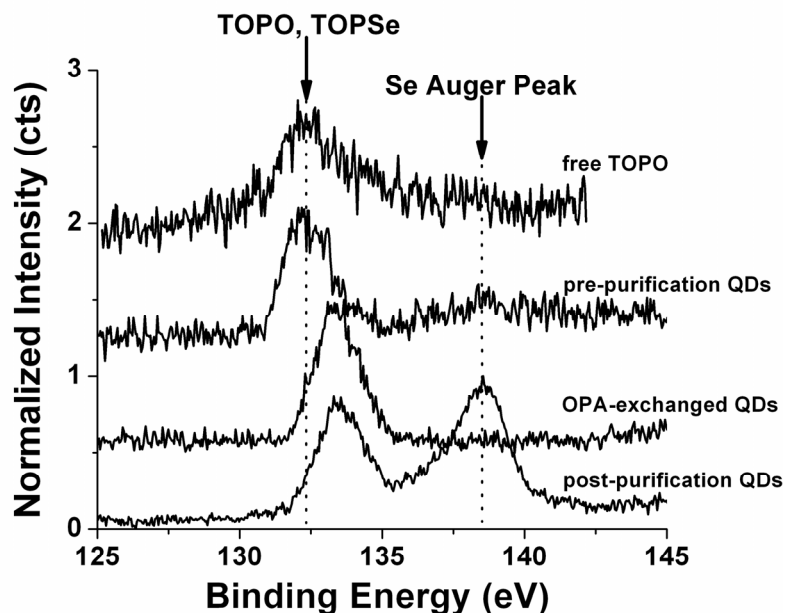


Figure S2. P(2p) region of the XPS spectra of the QDs used in this study (“post-purification QDs”), QDs with a high surface coverage of OPA formed by ligand exchange (“OPA-exchanged QDs”), QDs that have excess TOPO and TOPSe ligand because they have not yet been purified (“pre-purification QDs”), and free TOPO ligand (no QDs). The binding energy of P(2p) electrons shifts from 132.3 eV for TOPO and TOPSe (not shown) ligands to 133.2 eV for alkylphosphonate ligands. The peak at 138.5 eV is the Se Auger peak; it is also present in the spectrum of bulk CdSe that has not been exposed to phosphorous ligands.

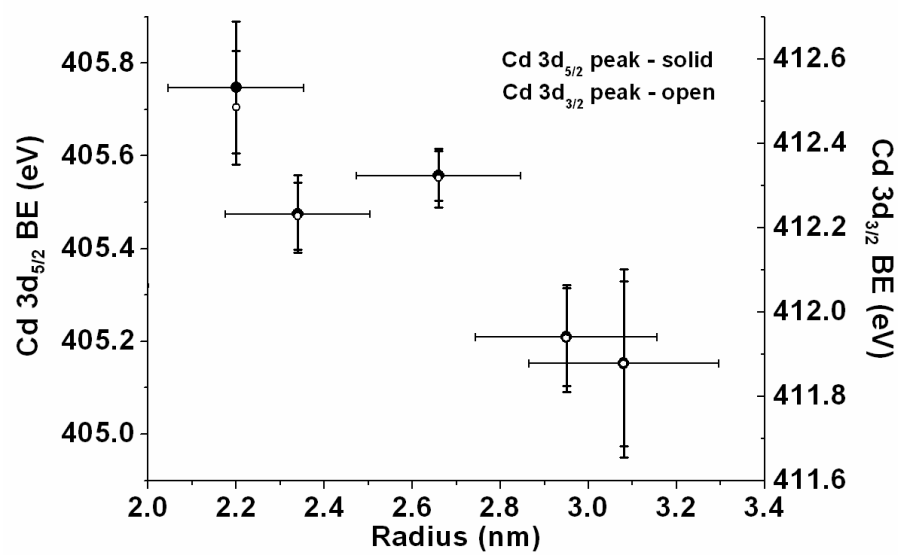


Figure S3. Binding energy of Cd(3d_{3/2}) and Cd(3d_{5/2}) showing the same trend in decreasing binding energy with increasing radius.

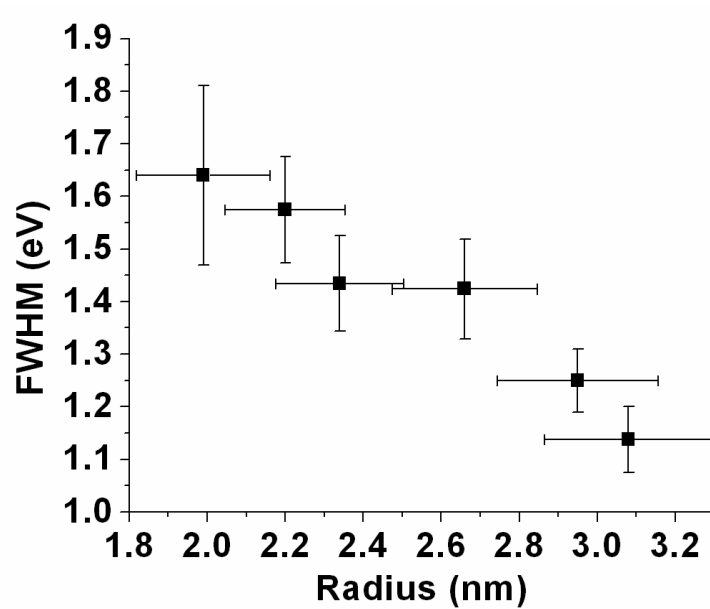


Figure S4. Linewidths for the Cd($3d_{3/2}$) peak, which shows the same trend in increasing linewidth for decreasing radius as the Cd($3d_{5/2}$).

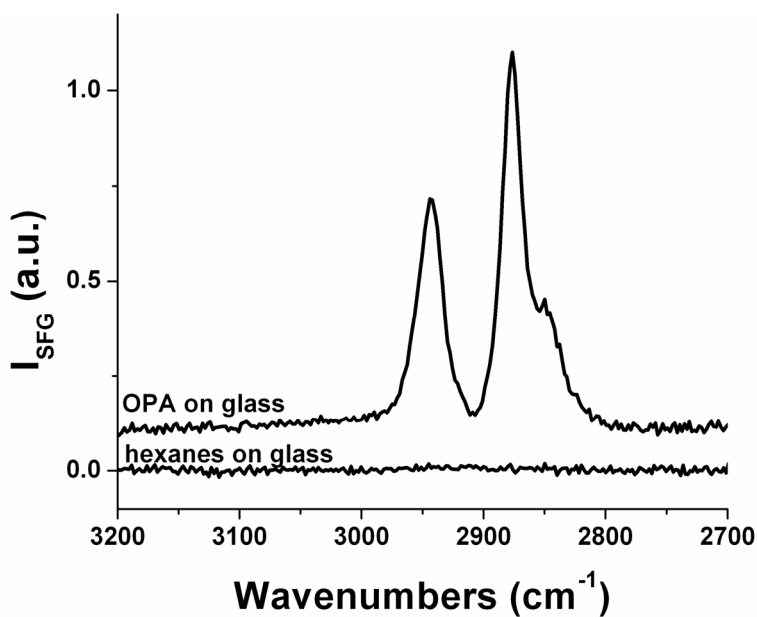


Figure S5. SFG spectra of OPA on plain glass. The OPA forms a more ordered layer on glass than on QDs.

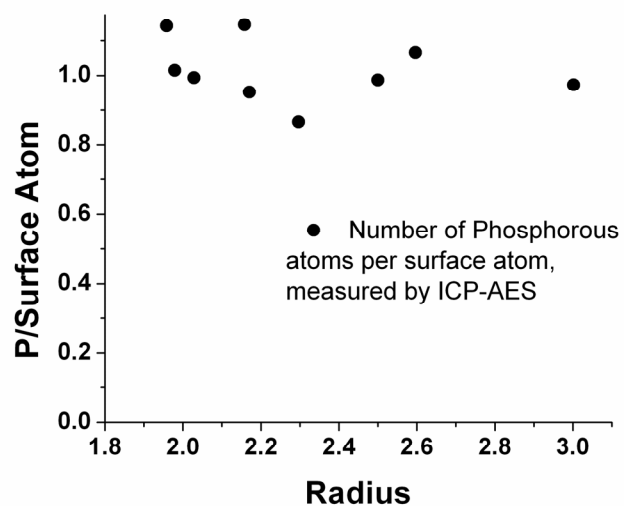


Figure S6. A plot of the number of phosphorous ligands per surface atom on various sizes of CdSe QDs. We calculated this ratio from the elemental concentrations of Cd, Se, and P, as measured by ICP-AES, and the number of surface atoms per QD, as estimated from the lattice parameters of bulk wurtzite CdSe, which introduces some error in the calculation since the surface is not crystalline.

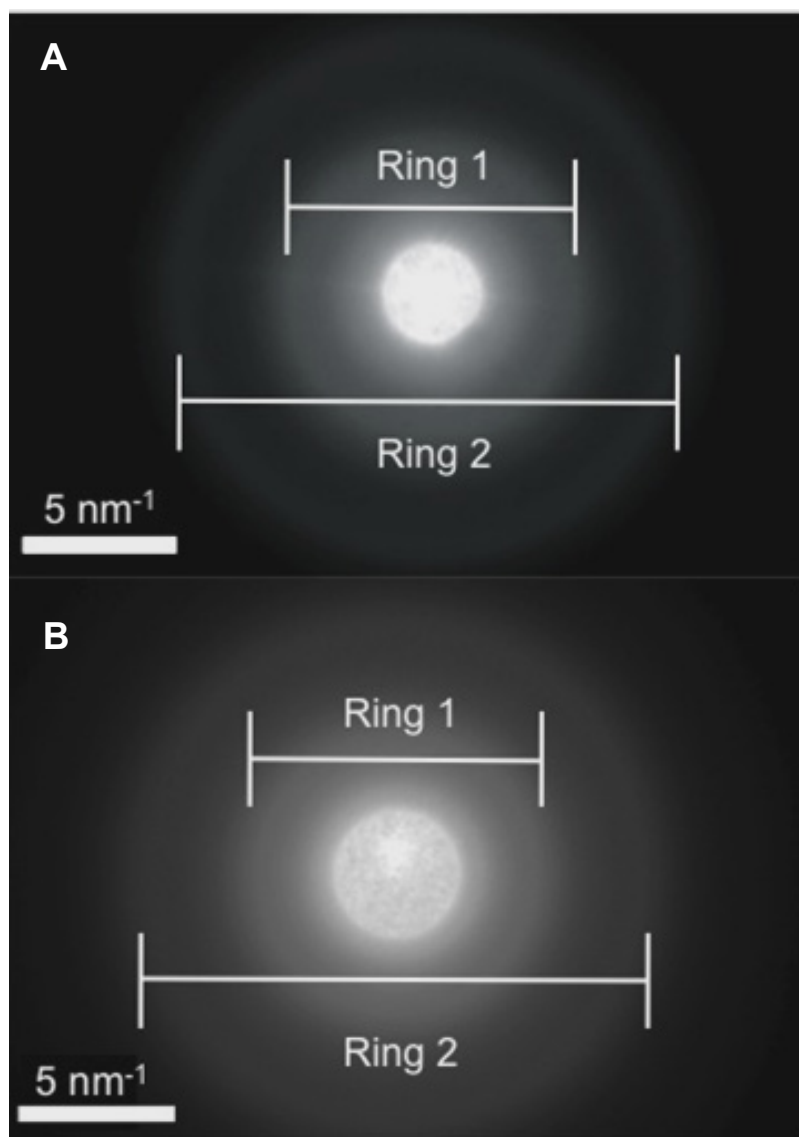


Figure S7. Representative electron diffractograms for ensembles of CdSe QDs with radii of 1.9 nm (**A**) and 2.3 nm (**B**). The two distinguishable diffraction rings correspond to lattice parameters of $2.20 \pm 0.07 \text{ \AA}$ (Ring 1) and $1.23 \pm 0.04 \text{ \AA}$ (Ring 2) for the 1.9-nm QDs and $2.20 \pm 0.05 \text{ \AA}$ and $1.22 \pm 0.04 \text{ \AA}$ for the 2.3-nm QDs. The values of the lattice parameters are the reciprocals of the average of measurements of the radii of the diffraction rings measured at seven different locations on a single sample. The reported errors are propagated from the standard deviations in the radius measurements. The electron beam used for the diffraction measurement illuminated a circular area of 1.02 \mu m^2 .

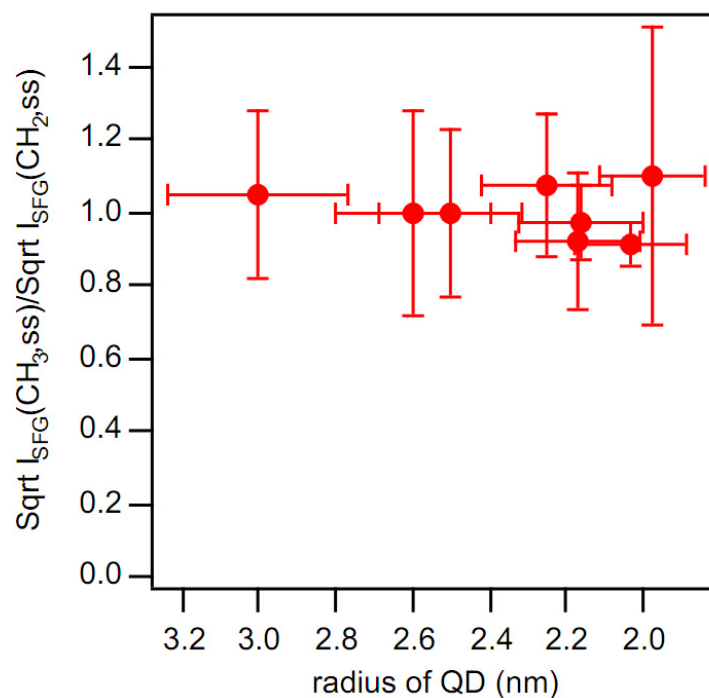


Figure S8. Ratio of the square root of the SFG intensities of CH₃ and CH₂ symmetric stretches, read directly from the raw spectra, for the ligands on the CdSe QDs synthesized with 90% TOPO, plotted against the radius of the QDs. The vertical error bars are the standard deviations of four measurements on one sample.

REFERENCES

- S1. Morris-Cohen, A. J., Donakowski, M. D., Knowles, K. E. & Weiss, E. A. *J. Phys. Chem. C* **2009** *114*, 897-906.